# Laboratory Formation of OBrO and Its Reactivity toward Ozone at 298 K

**Zhuangjie Li**

*Department of Atmospheric Sciences, University of Illinois at Urbana−Champaign, Urbana, Illinois 61801*

*Received: September 22, 1998; In Final Form: November 25, 1998*

Bromine dioxide, OBrO, has been formed in our laboratory using three methods in a discharge flow reactor: (1) O + $Br_2$; (2) Br + $O_3$; and (3) microwave discharge of a $Br_2/O_2$/He mixture. The OBrO radical was detected using a mass spectrometer at $m/e$ = 111/113. A new mechanism is proposed to account for the formation of the OBrO in these methods. The key to this mechanism is the self-reaction of vibrationally excited BrO. At 298 K, ground-state OBrO does not notably react with ozone, and an upper limit rate constant for the reaction of the ground-state OBrO with ozone was estimated to be $k_{13} \leq 5 \times 10^{-16}$ cm$^3$ molecule$^{-1}$ s$^{-1}$. The vibrationally excited OBrO, on the other hand, is at least 3 orders of magnitude more reactive toward ozone than the ground-state OBrO, with a rate constant of $k_{13a} = (5.4 \pm 2.7) \times 10^{-13}$ cm$^3$ molecule$^{-1}$ s$^{-1}$.

## I. Introduction

Recent field measurements showed the evidence for the possible presence of OBrO as a principal bromine-carrying species with an upper limit of around 20 pptv mixing ratio in a large part of the mid-latitude stratosphere at nighttime.[1,2] Although these recent field measurements need to be verified, they have sparked great interests in OBrO, which has received several investigations.[3−12] A primary question raised from this observation is what could be the source(s) of the OBrO radical. Another important question is if this species plays a role in affecting the stratospheric ozone.

The detailed mechanism for the atmospheric OBrO formation is still unclear. However, there have been several postulations regarding the laboratory formation of gaseous OBrO. Butkovskara et al.[4] observed the OBrO radical in the reaction of O atoms with $Br_2$, and suggested that the OBrO was formed via

$$O + Br_2 \rightarrow BrO + Br \qquad \Delta H_r(298\ K) = -11.7\ kcal\ mol^{-1}\ ^{13,14} \quad (1)$$

$$O + BrO + M \rightarrow OBrO + M \qquad \Delta H_r(298\ K) = -53.7\ kcal\ mol^{-1}\ ^{13-15} \quad (2)$$

By condensing the reaction products of O + $Br_2$ and Br + $O_3$ at −20 °C, Li et al.[16] observed the OBrO in their flow reactor upon warming up the products. The O + $Br_2$ system has become a source of OBrO for several spectroscopic studies of this radical.[8−10] Ratigan et al.[5,6] and Rowley et al.[16] observed OBrO in their BrO chemistry studies in which the BrO was produced by reacting Br with $O_3$, and they suggested the OBrO to be the product of the reaction of BrO with an excess of $O_3$:

$$Br + O_3 \rightarrow BrO + O_2 \qquad \Delta H_r(298\ K) = -32.2\ kcal\ mol^{-1}\ ^{13,14} \quad (3)$$

$$BrO + O_3 \rightarrow OBrO + O_2 \qquad \Delta H_r(298\ K) = -28.2\ kcal\ mol^{-1}\ ^{13-15} \quad (4)$$

Kölm et al.[5] suggested that OBrO may be produced from the BrO self-reaction:

$$BrO + BrO \rightarrow OBrO + Br \qquad \Delta H_r(298\ K) = 4.0\ kcal\ mol^{-1}\ ^{13-15} \quad (5)$$

but there has been no experimental observation reported for this formation channel. More recently, Deters et al.[18] observed OBrO as an impurity in their $BrONO_2$ sample synthesized by reacting excess $ClONO_2$ with $Br_2$, and ascribed the small amount of OBrO to heterogeneous or photolytic reactions in their storage vessel.

The reported detection of atmospheric OBrO suggests that the OBrO radical may exist in the form of gas in the atmosphere and potentially be involved in atmospheric chemistry. A major question concerning the OBrO radical would be whether and to what extent this radical interacts with the stratospheric ozone. The answer to this question will depend on the competition among the OBrO photo/thermal dissociation, the OBrO uptake by the atmospheric aerosols, and the OBrO reactions with ozone and other reactive species in the atmosphere. There has been very little information available regarding the atmospheric chemical processes involving OBrO, especially the interaction between OBrO and ozone. The assessment of the atmospheric role of OBrO requires close scrutiny of this species, and it is necessary to carry out laboratory studies of this radical. In this paper, we report several laboratory sources of the OBrO radical using discharge flow combined with the mass spectrometer (DF/MS) technique. The OBrO radical produced by these methods can be trapped and stored in a Pyrex vessel for later use. We also report our findings on the reactivity of OBrO toward ozone at 298 K using the same technique. As illustrated in our results, the trapped OBrO has very different chemical reactivity from the nontrapped OBrO when interacting with ozone.

## II. Experimental Section

The experimental apparatus for studying the OBrO sources and the reaction of OBrO with ozone is shown in Figure 1. The DF/MS technique has been well established and described previously,[19−21] and is only briefly discussed here. The reactor

10.1021/jp983827c CCC: $18.00 
Published on Web 02/17/1999

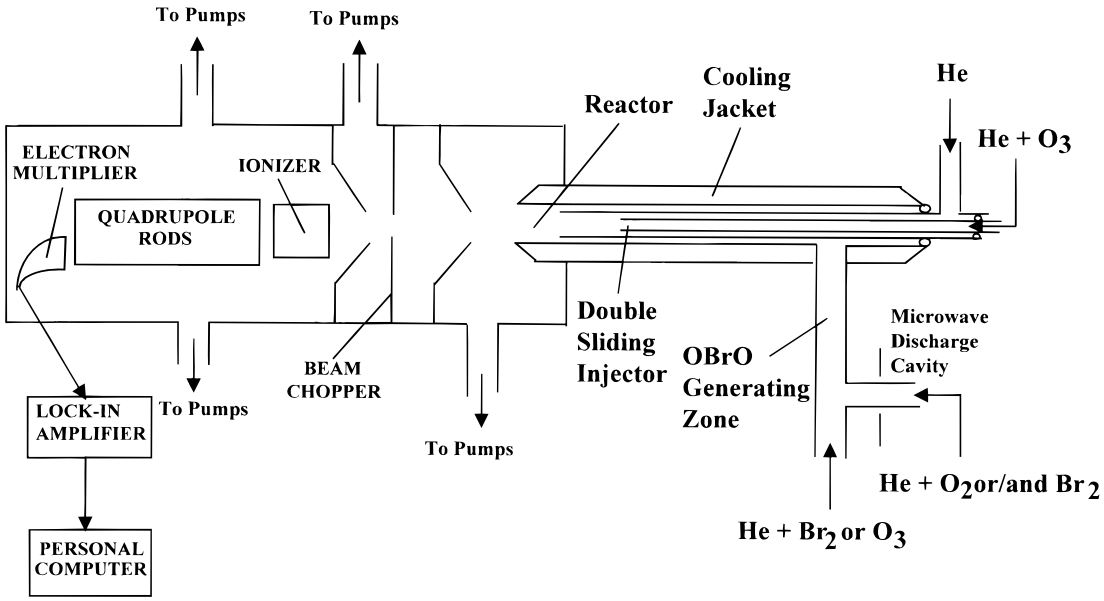


**Figure 1.** Experimental apparatus for OBrO formation and OBrO chemistry study.

consisted of a 100 cm long, 5.08 cm-i.d. Pyrex tube whose internal surface was covered with a layer of 0.05 cm thick TFE Teflon sheet to reduce the OBrO radical wall loss. The vacuum chamber for the discharge flow-modulated molecular beam mass spectrometer was a two-stage differentially pumped vacuum system with two 6 in. diffusion pumps with liquid nitrogen baffles, and the ultimate vacuum in the second stage was $<5 \times 10^{-10}$ Torr. A steady-state gas flow (total pressure of 1−10 Torr) was maintained in the flow tube with a 125 cfm mechanical pump (Edwards E2M175). Helium was introduced into the reactor as a carrier gas from the upstream of the reactor. The mean gas velocity in the flow tube varied between 500 and 1400 cm $s^{-1}$, resulting in residence times ranging from 160 to 60 ms in the 80 cm reaction zone. Kinetic measurements were carried out with the use of a double sliding injector which consisted of two concentric Pyrex tubes with the internal diameters of 9 mm and 12.7 mm, respectively. Contact times between the excess ozone and the limiting OBrO were varied by movement of the injector. A removable liquid nitrogen trap was placed downstream of the reactor in order to protect the vacuum pump from corrosive reactants and products.

Mass spectrometric detection of both reactants and products was conducted by continuous sampling at the downstream of the flow tube through a two-stage differentially pumped beam inlet system. Beam modulation was achieved with a 200 Hz tuning-fork-type chopper placed inside the second stage before the molecular beam enters the mass spectrometer (Extrel Model C50). Ion signals were sent to a lock-in amplifier (Model SR510, Stanford Research Systems, Inc.) that was referenced to the chopper frequency. The amplified analogue signals were digitized (Analogue Devices RTI/815) and recorded on a microcomputer. Under normal operational conditions, the detection limit for the apparatus was on the order of $(1-10) \times 10^9$ molecule $cm^{-3}$, depending on the individual species detected. Finally, mass spectra for both reactants and products were sampled, recorded, and digitized by an oscilloscope (Tektronix TDS 360); the spectra were then transferred to a personal computer for later analysis.

OBrO ($m/e = 111/113$) was generated by three methods: (1) reacting $Br_2$ with atomic oxygen which was produced by microwave discharge (OPTHOS INSTRUMENTS, INC. Model MPG-4) of an $O_2$/He mixture; (2) reacting ozone with atomic Br generated by microwave discharge of a $Br_2$/He mixture; and (3) microwave discharging a $Br_2/O_2$/He mixture. The signal intensity ratio of $m/e = 111$ ($O^{79}BrO^+$) to $m/e = 113$ ($O^{81}BrO^+$) was found to be close to 1, which was consistent with the natural relative abundance of 1.03 for $^{79}Br/^{81}Br$.[22]

In method 1, $(1-5) \times 10^{13}$ molecule $cm^{-3}$ of $Br_2$ carried by 250 sccm of helium (measured using flow controller from Hasting Instruments) reacted with atomic oxygen generated by microwave discharge of $(5-30) \times 10^{13}$ molecule $cm^{-3}$ $O_2$ carried by 1000 sccm of He. The reaction was confined in a Pyrex tube with an o.d. of 1.27 cm. The total pressure in the reaction zone was 1−2 Torr, and the reaction time for the generation of OBrO was about a few milliseconds. It was found that too much $Br_2$ (e.g., $[Br_2] \geq 3 \times 10^{14}$ molecule $cm^{-3}$) reduced the OBrO radical production.

In method 2, $(9-25) \times 10^{13}$ molecule $cm^{-3}$ of $O_3$ carried by 10−100 sccm of He reacted with atomic bromine produced by microwave discharge of $Br_2$ in the Pyrex tube. The concentration of $Br_2$ was $(1-3) \times 10^{14}$ molecule $cm^{-3}$, and the $Br_2$ was carried by 800−1000 sccm of He. Although OBrO was observed in this synthesis method, it did not generate substantial amounts of OBrO. As discussed in the next section, this may be due to the secondary reaction which occurred in the tube, which removed the OBrO radical rapidly.

In method 3, $(2-6) \times 10^{14}$ molecule $cm^{-3}$ of $O_2$ was mixed with $(1-5) \times 10^{13}$ molecule $cm^{-3}$ of $Br_2$, and the mixture was carried by 1000−1300 sccm of He through the microwave discharge device. On the basis of $Br_2$ mass spectral signal intensity change before and after turning on the microwave discharge device, about 25% of the $Br_2$ was consumed with a discharge power of 30 W. The maximum production of OBrO was obtained by slightly varying the concentrations of either $Br_2$ or $O_2$. On the basis of our experience, it was critical to synthesize the OBrO under low-pressure conditions (∼1 Torr) since the OBrO seemed to be quickly removed by secondary reactions under higher pressures. In general, method 3 gave the highest OBrO yields. Method 1 also produced substantial amounts of OBrO, but method 2 offered a poor OBrO radical production yield.

The operational conditions of our mass spectrometer were then optimized for the best detection of the parent ion of the OBrO radical. It was found that the mass signal for the OBrO

parent ion was maximized with an electron impact energy of 40.0 eV and an emission current of 3.0 mA. The OBrO radical is fragmented in the ionization region of the mass spectrometer when bombarded by the high-energy electrons, producing $BrO^+$ ($m/e = 95$) as its daughter ion. With our mass spectrometer operational conditions set above, the ratio of the peak parent ion signal ($S_{111}$) to the peak daughter ion signal ($S_{95}$), $S_{111}/S_{95}$, was found to be $0.50 \pm 0.03$ for the trapped OBrO (the preparation of the trapped OBrO is discussed in the next paragraph). This ratio was not significantly altered under the electron impact energy in the range of 30.0−40.0 eV. Finally, the absolute OBrO concentration was calibrated by chemically converting the trapped OBrO into $NO_2$ with an excess of NO ($\sim 5 \times 10^{14}$ cm$^{-3}$). The rate constant at 298 K for the reaction of the trapped OBrO with NO:

$$\mathrm{OBrO} + \mathrm{NO} \rightarrow \mathrm{BrO} + \mathrm{NO_2}$$
$$\Delta H_r(298\ \mathrm{K}) = -27.8\ \mathrm{kcal\ mol^{-1}}\ ^{13-15} \quad (6)$$

was determined to be $k_6 = (1.77 \pm 0.32) \times 10^{-12}$ cm$^3$ molecule$^{-1}$ s$^{-1}$ in a separate study in our laboratory.[23] The BrO produced from reaction 6 can further react with NO:

$$\mathrm{BrO} + \mathrm{NO} \rightarrow \mathrm{Br} + \mathrm{NO_2}$$
$$k_7 = 2.1 \times 10^{-11}\ \mathrm{cm^3\ molecule^{-1}\ s^{-1}}\ ^{25} \quad (7)$$

Since reaction 7 was much faster than reaction 6, the BrO was converted into $NO_2$ within 1 ms in the reactor. Thus, each OBrO participating in reaction 6 was assumed to generate two $NO_2$ molecules. The conversion factors were determined from the ratio of the change in $NO_2$ ion signal at $m/e = 46$, $S_{46}$, to the change in the OBrO radical signal at $m/e = 111$, $S_{111}$, ($\Delta S_{46}/\Delta S_{111} = 4.6 \pm 0.2$). The radical calibrations were then obtained from absolute calibrations of the mass spectrometer at $m/e = 46$ using the known concentration of $NO_2$. The detection limit for the OBrO radical was $8 \times 10^9$ molecule cm$^{-3}$.

The OBrO radicals produced in methods 1 and 3 can be collected by trapping the reaction products into a Pyrex sample cell in the temperature range from −35 to −45 °C. A brown-yellow colored solid substance was formed as a layer coated on the inner surface of the cell after synthesis for about 60 min. Mass spectroscopic examination of the gaseous species evaporated from this initially collected sample mixture identified feature signals for $Br_2$ ($m/e = 158/160/162$), BrO ($m/e = 95/97$), OBrO ($m/e = 111/113$), and $Br_2O$ ($m/e = 174/176/178$). Since the uptake coefficient of BrO on the Pyrex surface was expected to be small, and $Br_2$ has a vapor pressure of greater than 1 Torr at −45 °C, both BrO and $Br_2$ were unlikely to be condensed into a solid at the trapping temperatures and the total pressure of 1 Torr. Thus the sample mixture contained mainly OBrO and $Br_2O$. The BrO and $Br_2$ signals could be due either to thermal decomposition or to self-reaction of the sample mixture during the transport of the sample from the sample cell to the reactor, or due to the fragmentation of the OBrO and $Br_2O$ in the ionization region of the mass spectrometer. When the sample cell was placed in a bath at 0 °C and pumped for about 90 min, a white-yellow colored solid layer was left on the internal surface of the cell. Examination of the gaseous sample evaporated from the white-yellow solid layer still revealed a mixture of $Br_2$, BrO, OBrO, and $Br_2O$. But the signal intensity ratio of OBrO to $Br_2O$, $S_{111}/S_{176} = 2.5$, was higher than that ($S_{111}/S_{176} = 0.5-1$) before pumping, indicating that an OBrO sample with higher purity was obtained. The signal ratio, $S_{111}/S_{95}$, appeared to be constant after the pumping. Thus the signal levels at $m/e = 111$ and 95 did not seem to be affected by the $Br_2O$ that remained, and the white-yellow solid in the sample cell could then last for several hours in providing $\sim 5 \times 10^{12}$ molecule cm$^{-3}$ of OBrO for the flow reactor.

The investigation of the OBrO reactivity toward ozone was carried out by monitoring the decay of OBrO radical as a function of reaction time in the presence of excess ozone. When a decay was observed, the rate constant for the reaction of OBrO with ozone can be obtained using the well-known steady-state flow tube method,[19−21] in which the pseudo-first-order rate constant for the reaction was given as[20]

$$k = -v\frac{\mathrm{a}}{\mathrm{d}z}(\ln[\mathrm{OBrO}]) \quad \text{(I)}$$

where $v$ was the carrier gas flow velocity and $z$ the injector position. However, the observed decays needed to be corrected for the axial diffusion according to eq II,

$$k' = k\left(1 + k\frac{D}{\mathrm{v}^2}\right) + k_p \quad \text{(II)}$$

where $D$ was the estimated diffusion coefficient and $k_p$ the first-order loss of OBrO on the outside surface of the sliding injector.[21,23] By varying the $O_3$ concentrations, different decay rate constants were collected. When the pseudo-first-order decay rate was plotted as a function of the initial $O_3$ concentration, $[O_3]_0$, the slope of the fitted straight line yielded the bimolecular rate constant for reaction of OBrO with ozone at the temperature of the reactor, which was 298 K.

The gases used in this work were obtained mainly from S. J. Smith Welding Supply: He, 99.999%; $O_2$, 99.999%; NO, 99%; and $NO_2$, 99.5%. The $NO_2$ sample was purified by two methods: (1) multiple low-temperature (195 K) distillations to remove the volatile NO, and (2) addition of $O_2$ to the sample in order to convert the NO impurity into $NO_2$. All other gases were used as received. $Br_2$ > 99% was obtained from Fisher Scientific. $O_3$ was produced by an ozone gas generator (Pacific Ozone Technology L21) and stored on silica gel at 195 K. During the experiments, $O_3$ was maintained at 195 K and bubbled into the reactor with a measured flow of He (10−500 sccm). A cold trap cooled by liquid nitrogen was placed before the inlet of the mechanical pump to avoid the contamination of the pump by the corrosive chemicals. For experiments involving $O_3$, the ozone was catalytically converted into $O_2$ by passing it through a heated U-tube containing copper fibers as a catalyst before arriving at the trap. It was found that when the U-tube temperature reached 200−250 °C, >99% of the ozone was converted and very little ozone was trapped at liquid nitrogen temperature.

## III. Results and Discussion

**A. Formation of the OBrO Radical.** Figure 2 shows the mass spectra illustrating the production of the OBrO radical from the O + $Br_2$ system (Figure 2a), the Br + $O_3$ system (Figure 2b), and microwave discharge of the $Br_2/O_2$/He mixture (Figure 2c). It can be seen clearly that both BrO and OBrO were produced in these systems. The peak pairs at $m/e = 95/97$ and $m/e = 111/113$ with similar intensity represent the $^{79}$Br

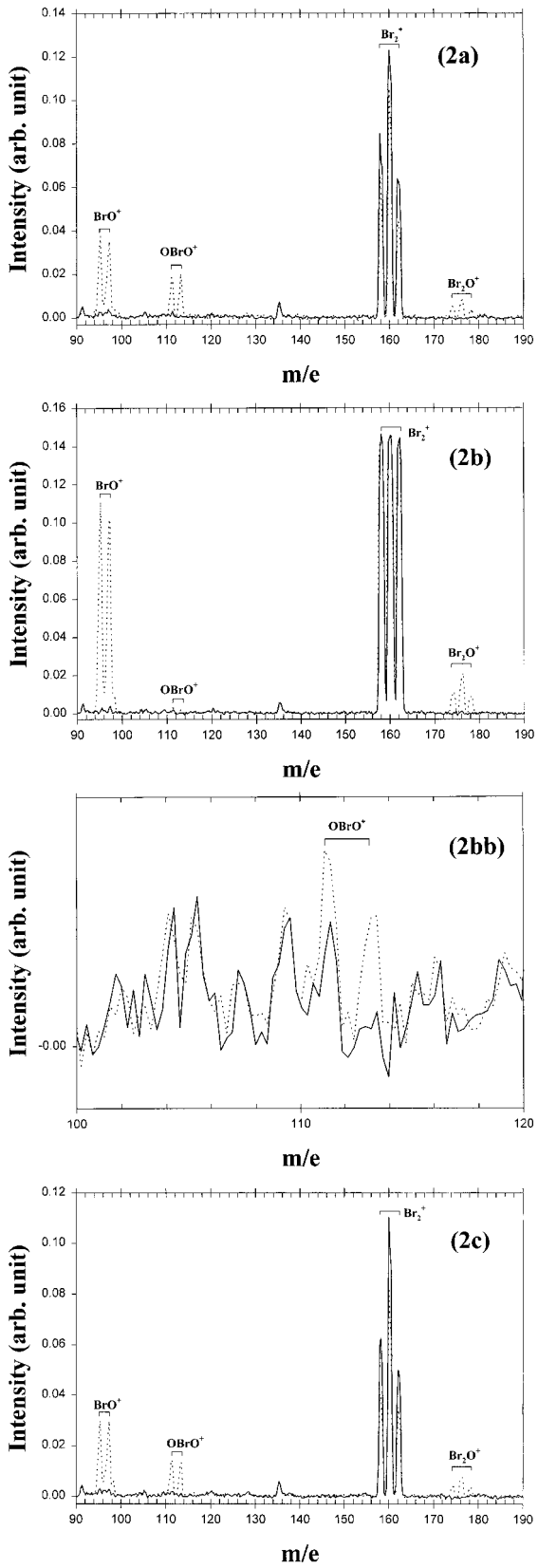


**Figure 2.** Mass spectra from three OBrO generating methods: (a) $Br_2 + O$, $[Br_2]_0 = 1.2 \times 10^{13}$ molecule cm$^{-3}$, and $[O_2]_0 = 3.2 \times 10^{14}$ molecule cm$^{-3}$; (b) $Br + O_3$, $[Br_2]_0 = 9.1 \times 10^{13}$ molecule cm$^{-3}$, and $[O_3]_0 = 2.6 \times 10^{14}$ molecule cm$^{-3}$, (bb) a zoom of Figure 2b in the mass range of $m/e = 100-120$; (c) microwave discharge of $Br_2/O_2$/He mixture: $[Br_2]_0 = 1.2 \times 10^{13}$ molecule cm$^{-3}$, and $[O_2]_0 = 1.7 \times 10^{14}$ molecule cm$^{-3}$. The solid-line waveforms were taken before turning on the microwave discharge device, and the dotted-line waveforms were taken after the microwave discharge device was turned on.

and $^{81}Br$ isotopes in both $BrO^+$ and $OBrO^+$. The peaks at $m/e = 111/113$ do not seem to be due to the fragmentation of other higher bromine oxides since no other higher bromine oxide parent ions such as $BrO_3$ ($m/e = 127/129$) and $(BrO)_2$ ($m/e = 190$) were observed in the spectra. The assignment of the peaks at $m/e = 111/113$ to the OBrO radical was confirmed by FTIR spectral study of the species, in which the products prepared by methods 1 and 3 were trapped at $-30$ to $-45$ °C and warmed to ice temperature then sent to an FTIR spectrometer.[24] The IR spectrum taken for the products matches that reported by Miller et al.[8]

A small amount of $Br_2O$ ($m/e = 174/176/178$) was also observed in all three OBrO synthesis methods (see Figure 2). Rowley et al.[17] suggested that the $Br_2O$ is formed by reaction of Br with BrO:

$$Br + BrO + M \rightarrow Br_2O + M$$
$$\Delta H_r(298\ K) = -29.7\ kcal\ mol^{-1}\ ^{13,14,25} \quad (8)$$

It is also possible that the observed $Br_2O$ could result from the reaction of BrO with OBrO:

$$BrO + OBrO \rightarrow Br_2O + O_2$$
$$\Delta H_r(298\ K) = -35.6\ kcal\ mol^{-1}\ ^{13,15,25} \quad (9)$$

The formation of $Br_2O$ from reaction 9 would require either a four-center or a five-center collision complex transition state breaking two Br−O bonds while forming one Br−O bond and one O−O bond, and reaction 9 would not be likely to be fast. However, if both BrO and OBrO were in vibrationally excited state, as suggested in later discussion of this paper, reaction 9 could play a role in the production of the small amount of $Br_2O$.

In both methods 1 and 3, the $Br_2O$ formed above could interact with atomic oxygen:

$$O + Br_2O \rightarrow BrO + BrO$$
$$\Delta H_r(298\ K) = -28.0\ kcal\ mol^{-1}\ ^{13,14,25} \quad (10a)$$
$$\rightarrow OBrO + Br$$
$$\Delta H_r(298\ K) = -24.0\ kcal\ mol^{-1}\ ^{13,15,25} \quad (10b)$$

and reaction 10b could provide a possible alternative pathway for the production of OBrO. To examine if the reaction 10b would contribute to the OBrO formation in methods 1 and 3, we carried out a separate experiment to investigate the interaction between O and $Br_2O$. The $Br_2O$ used in this experiment was produced by reacting $Br_2$ with HgO:[26]

$$2Br_2 + HgO \rightarrow Br_2O + HgBr_2 \quad (11)$$

in which the $Br_2O$ synthesis method was slightly modified to obtain a stable constant flow of $Br_2O$.[24] BrO was found to be the only product and no OBrO was found when 95% of $\sim(5-10) \times 10^{12}$ molecule cm$^{-3}$ $Br_2O$ reacted with atomic oxygen, indicating that reaction 10b could not be the source of the OBrO in both methods 1 and 3.

It seems that the OBrO radical can be readily generated under our experimental conditions, but how the OBrO was formed needs more understanding. The atomic oxygen was involved in both methods 1 and 3, and reaction 1 followed by reaction 2 leading to the OBrO formation was thermodynamically feasible. However, this reaction scheme could not satisfactorily explain the present observation of OBrO formation since reaction 2 was a three-body process that was not favored in our reactor maintaining a total pressure of 1 Torr. One possible mechanism

for the OBrO formation was that the OBrO was formed by the reaction of O atoms with BrO heterogeneously on the reactor wall. This would require that either O or BrO be adsorbed on the Pyrex wall in the OBrO generating zone for collision of these two species. Since neither of these species had a large sticking coefficient on the Pyrex surface at 298 K, the likelihood for the heterogeneous formation of OBrO in our reactor should be small. But the heterogeneous OBrO formation mechanism must be tested. In one experiment, the OBrO generating zone, i.e., the O + $Br_2$ zone, was heated to 513 K to reduce the adsorption of both O and BrO on the Pyrex wall. It was found that the production of OBrO was hardly affected in the temperature range 298−513 K, indicating an insignificant contribution of the heterogeneous process to the OBrO formation in method 1. Furthermore, since the concentration of bromine was always in excess over that of atomic oxygen, the oxygen atoms were basically titrated by the $Br_2$ and there were very few O atoms left to combine with BrO to form OBrO. In fact, there was no atomic oxygen involved in method 2, yet the OBrO was still observed, indicating that reaction 2 was not the primary OBrO source, and that there was an alternative mechanism leading to the OBrO formation.

There were two additional possible reactions in the OBrO generating zone that could give rise to the OBrO production without involving atomic oxygen, i.e., the reaction of ozone with BrO (reaction 4) and the BrO self-reaction (reaction 5). There has been evidence of OBrO formation from reaction 4,[17] but this process has been known to be a slow and low OBrO yield channel and hence cannot account for the large OBrO production in our reactor. In our methods 1 and 3, a possible pathway resulting in OBrO generation without O atom participation would be the BrO self-reaction (reaction 5). On the basis of thermodynamic data,[13−15] reaction 5 is endothermic by ∼4 kcal $mol^{-1}$, and this reaction channel is not thermodynamically favored for producing OBrO. In fact, the ground-state BrO self-reaction has been known to form Br, $Br_2$, and $O_2$ as products and there has been no report on the observation of OBrO as a product from reaction 5.[27−33] Thus the OBrO formation cannot be due to the BrO self-reaction involving radicals in the ground state. The BrO radical generated from reaction 1 could, however, be vibrationally excited (signified as $BrO^{‡}$). We noticed that there was 11.7 kcal $mol^{-1}$ of heat released from the reaction 1, which was assumed to be equally partitioned between the products, BrO and Br. On the basis of this consideration and assumption, the vibrationally excited BrO would carry more energy than the ground-state BrO by 5.8 kcal $mol^{-1}$. This extra vibrational energy adding to the BrO reactant(s) would change reaction 5 from an endothermic into an exothermic process so that the reaction becomes thermodynamically feasible:

$$BrO^{‡} + BrO \rightarrow OBrO + Br \qquad \Delta H_r(298\ K) = -1.8\ kcal\ mol^{-1}\ ^{13-15} \quad (5a)$$

$$BrO^{‡} + BrO^{‡} \rightarrow OBrO + Br \qquad \Delta H_r(298\ K) = -7.7\ kcal\ mol^{-1}\ ^{13-15} \quad (5b)$$

It is conceivable that the majority of the BrO from reaction 1 was quenched to the ground state, since the collision frequency of the molecule in our reactor was on the order of $10^7\ s^{-1}$, and only a portion of $BrO^{‡}$ made its way to form OBrO. In the case of method 3, since a mixture of $Br_2/O_2$/He was microwave discharged, both atomic bromine and oxygen were produced. The bromine atom produced by either reaction 1 or microwave discharge could then combine with the oxygen atom to form

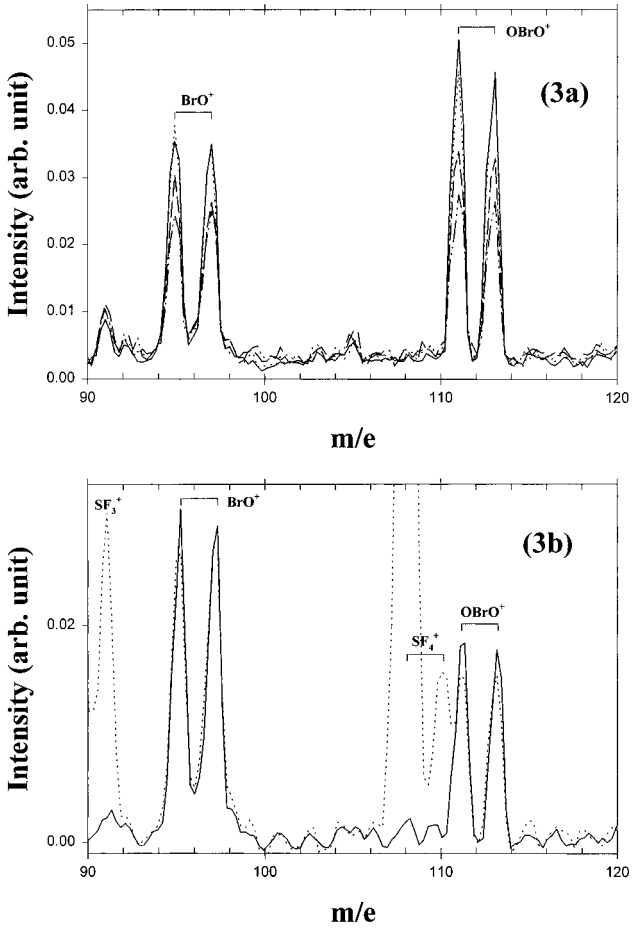


**Figure 3.** Mass spectra of the O + $Br_2$ system before and after addition of Ar and $SF_6$. (a) $[Br_2]_0 = 1.6 \times 10^{13}$ molecule $cm^{-3}$, $[O_2]_0 = 3.0 \times 10^{14}$ molecule $cm^{-3}$, and [Ar] = 0.0 (solid line); $0.7 \times 10^{16}$ (dotted line); $2.0 \times 10^{16}$ (dashed line), and $3.1 \times 10^{16}$ (double dotted-dashed line) molecule $cm^{-3}$. (b) $[Br_2]_0 = 1.2 \times 10^{13}$ molecule $cm^{-3}$, $[O_2]_0 = 2.0 \times 10^{14}$ molecule $cm^{-3}$, and $[SF_6] = 5 \times 10^{14}$ molecule $cm^{-3}$.

$BrO^{‡}$:

$$Br + O \rightarrow BrO^{‡} \qquad \Delta H_r(298\ K) = -51.9\ kcal\ mol^{-1}\ ^{13,14} \quad (12)$$

As a result, in addition to reaction 1 there would be more vibrationally excited BrO available for reactions 5a and 5b, and the OBrO radical was more readily produced.

To test the hypothesis of the vibrationally excited BrO self-reaction leading to the formation of OBrO, argon and $SF_6$ were introduced into the O + $Br_2$ system to see if there were any effects on the production of the OBrO radical. Figure 3 shows the mass spectrum before (the solid line) and after the addition of $(0.7-3.1) \times 10^{14}$ molecule $cm^{-3}$ and $\sim 5 \times 10^{14}$ molecule $cm^{-3}$ of Ar and $SF_6$, respectively, into the reactor containing the O + $Br_2$ system. It can be seen that the OBrO decreased upon addition of Ar (Figure 3a) or $SF_6$ (Figure 3b). Assuming that the $SF_6$ did not react with OBrO, the decrease of OBrO could be due to the quenching of the $BrO^{‡}$ by both Ar and $SF_6$, causing a reduction of the total amount of the $BrO^{‡}$ in the O + $Br_2$ system, and hence a reduction of the OBrO production from reactions 5a and 5b.

**B. Reactivity of OBrO toward Ozone.** The interaction between ozone and the OBrO radical at 298 K was investigated in the present work for two OBrO cases: (1) the OBrO radicals produced by methods 1 and 3 were trapped and then evaporated (referred to as trapped OBrO, or ground-state OBrO) to react

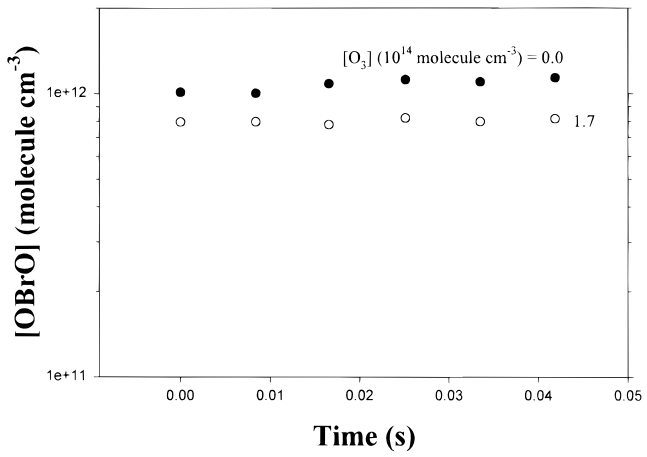


**Figure 4.** Temporal behavior of the trapped OBrO in the absence (solid circle) and the presence (open circle) of ozone.

with ozone, and (2) the OBrO radicals produced by methods 1 and 3 were directly introduced into the reactor (referred as nontrapped OBrO) to react with ozone. Our data revealed a remarkably different reactivity feature for OBrO toward ozone in these two cases. Figure 4 shows the temporal behavior of the trapped OBrO both in the absence and in the presence of ozone. Essentially no decay was observed when $1.7 \times 10^{14}$ molecule $cm^{-3}$ of ozone was added to the reactor containing $(1-2) \times 10^{12}$ molecule $cm^{-3}$ of ground state OBrO, suggesting that the OBrO was not notably reactive to ozone molecule. No prominent OBrO decay was observed even when the ozone concentration was increased to $(5-10) \times 10^{15}$ molecule $cm^{-3}$. The rate constant for the reaction of ground-state OBrO with $O_3$

$$\mathrm{OBrO} + \mathrm{O_3} \rightarrow \text{products} \qquad (13)$$

was then estimated to be $k_{13} \leq 5 \times 10^{-16}$ $cm^3$ $molecule^{-1}$ $s^{-1}$.

However, without trapping the OBrO radical, an OBrO decay was observed upon adding ozone molecules into the reactor. Figure 5 shows the mass spectra of the O + $Br_2$ system both in the absence and in the presence of ozone. It can be seen that when $(1.7-18) \times 10^{13}$ molecule $cm^{-3}$ of ozone was added to the O + $Br_2$ system, the OBrO was greatly suppressed, suggesting that the OBrO species was consumed by the ozone molecules. This observation was very different from the trapped OBrO reaction with ozone. In a separate experiment in which NO was used to react with both the trapped and nontrapped OBrO, we found that the nontrapped OBrO reacts much faster than the trapped OBrO.[23] These observations suggest that the OBrO produced in situ has much higher reactivity than the trapped OBrO. It is unclear why the trapped and nontrapped OBrO behave so differently when reacting with ozone and other species. One possible explanation is that, like $BrO^{‡}$, the OBrO formed by reactions 5a and 5b in both methods 1 and 3 could also be vibrationally excited (signified as $OBrO^{‡}$), which increased the reactivity of OBrO toward ozone.

The observed increase of BrO upon addition of ozone to the O + $Br_2$ system in Figure 5b could be attributed to two chemical processes: (1) reaction of ozone with bromine atom (i.e., reaction 3) which was produced from reaction 1, and (2) reaction of ozone with $OBrO^{‡}$:

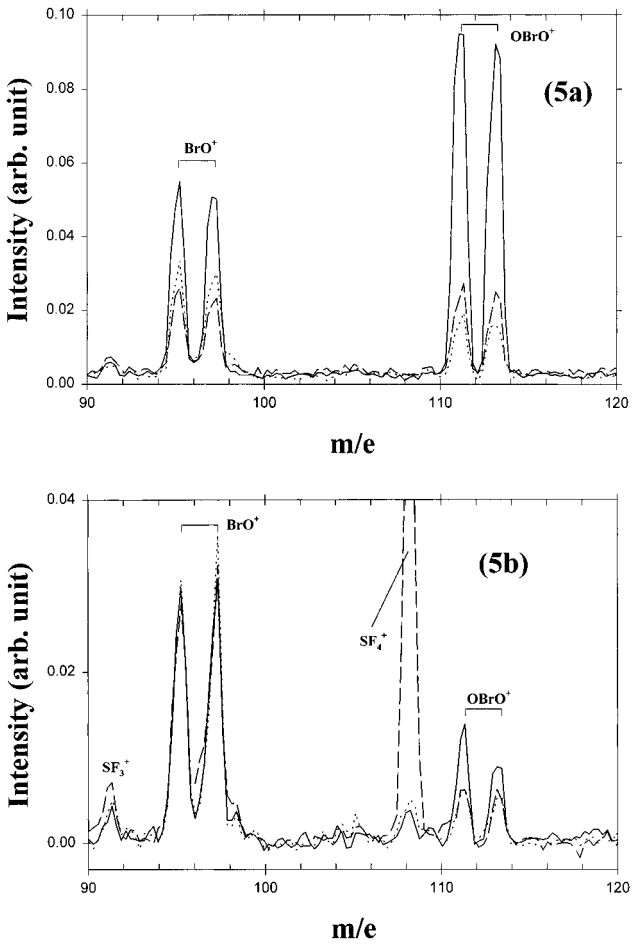


**Figure 5.** Mass spectra of the O + $Br_2$ system before (solid line) and after (dotted line) addition of ozone. (a) $[Br_2]_0 = 1.6 \times 10^{13}$ molecule $cm^{-3}$, $[O_2]_0 = 2.0 \times 10^{14}$ molecule $cm^{-3}$, and $[O_3] = 1.8 \times 10^{14}$ molecule $cm^{-3}$; $3.2 \times 10^{16}$ molecule $cm^{-3}$ of Ar was then added to the system (dashed line). (b) $[Br_2]_0 = 1.2 \times 10^{13}$ molecule $cm^{-3}$, $[O_2]_0 = 2.6 \times 10^{14}$ molecule $cm^{-3}$, and $[O_3] = 1.7 \times 10^{13}$ molecule $cm^{-3}$; $1 \times 10^{14}$ molecule $cm^{-3}$ of $SF_6$ was then added to the system (dashed line).

$$\mathrm{OBrO^{‡}} + \mathrm{O_3} \rightarrow \mathrm{BrO} + 2\mathrm{O_2}$$
$$\Delta H_r(298\ \mathrm{K}) < -40.0\ \mathrm{kcal\ mol^{-1}}\ ^{13-15} \qquad (13a)$$
$$\rightarrow \mathrm{BrO_3} + \mathrm{O_2}$$
$$\Delta H_r(298\ \mathrm{K}) < -15.8\ \mathrm{kcal\ mol^{-1}}\ ^{13,15,34} \qquad (13b)$$

Since no parent ion of $BrO_3$ ($m/e$ = 127/129) was observed from reaction 13b, it seemed that BrO should be the dominant, if not the only, product for the reaction of $OBrO^{‡}$ with ozone.

When $3.2 \times 10^{16}$ molecule $cm^{-3}$ of Ar and $1 \times 10^{14}$ molecule $cm^{-3}$ of $SF_6$ were added to the reactor containing both $OBrO^{‡}$ and ozone, an increase in OBrO signal was observed (see Figure 5, parts a and b). One explanation for this observation is that both Ar and $SF_6$ quenched a portion of $OBrO^{‡}$ which would have reacted with ozone. Since the ground-state OBrO was much less reactive to ozone, the quenched portion of $OBrO^{‡}$ then can give rise to the increase of the OBrO radical in the reactor.

Although the vibrationally excited BrO and OBrO are proposed to explain our experimental observations, it is unclear which vibrational level(s) could have been populated for both $BrO^{‡}$ and $OBrO^{‡}$, which would drive reactions 5a, 5b, and 13a. More studies are needed to obtain the detailed information regarding these radicals in the vibrationally excited state.

The kinetics for the reaction of $OBrO^{‡}$ with ozone was then studied under a pseudo-first-order condition in which the ozone

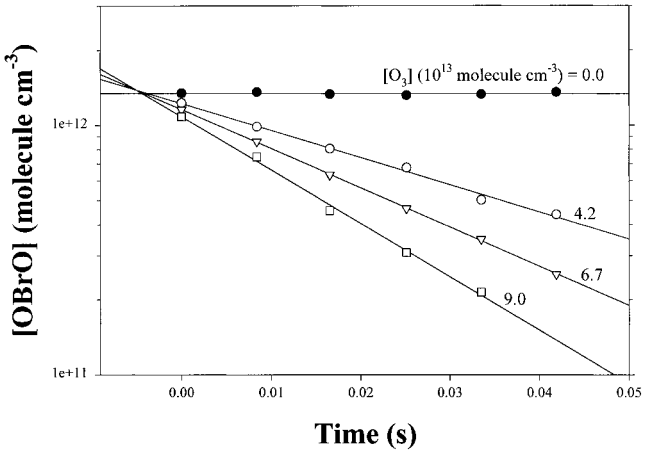


**Figure 6.** Typical decay of the nontrapped OBrO in the presence of ozone.

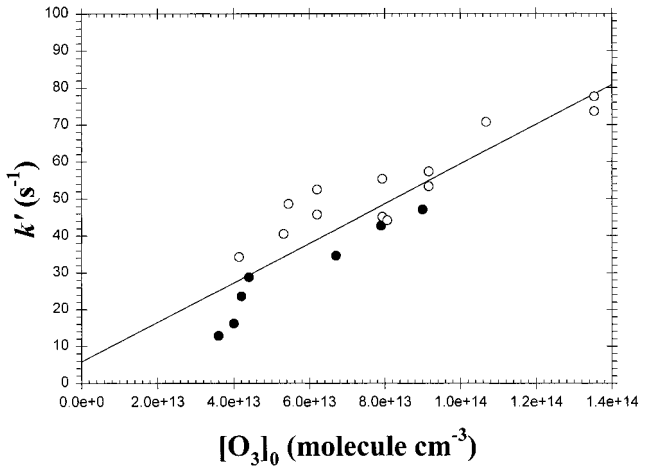


**Figure 7.** Pseudo-first-order decay rate of nontrapped OBrO vs $[O_3]_0$. The data points in open circle were taken using $OBrO^‡$ prepared by method 1 and that in filled circle by method 3. The slope of the fitted straight line through all data yield a rate constant of $k_{13a} = (5.4 \pm 2.7) \times 10^{-13}$ cm$^3$ molecule$^{-1}$ s$^{-1}$ for reaction 13a.

concentration was in excess over that of $OBrO^‡$. Figures 6 and 7 show a typical decay of the nontrapped OBrO as a function of reaction time in the presence of different ozone concentrations, and a pseudo-first-order decay rate measured as a function of the ozone concentration, respectively. Since there was no possible way to measure $OBrO^‡$ selectively with a mass spectrometer, the data in Figures 6 and 7 illustrate the decay of $[OBrO + OBrO^‡]$ with majority of $\frac{d}{dt}[m/e = 111]$ due to the loss of $OBrO^‡$. Note that the kinetics data collected by using method 1 were consistent with that collected by using method 3 as the $OBrO^‡$ source, and the $OBrO^‡$ first-order decay rate varies $10-78$ s$^{-1}$ when the ozone concentration changes in the range $(2-13) \times 10^{13}$ molecule cm$^{-3}$. The bimolecular rate constant for reaction 13a is then determined, by measuring the slope of the fitted straight line through all data points, to be $k_{13a} = (5.4 \pm 2.7) \times 10^{-13}$ cm$^3$ molecule$^{-1}$ s$^{-1}$, where the quoted error is taken as $2\sigma$ and reflects the scatter of the data and the uncertainty of experimental parameters such as temperature, flow rate, pressure, and ozone concentration. The rate constant for reaction 13a appears to be at least 3 orders of magnitude greater than that of reaction 13, suggesting a significant enhancement of the reactivity toward ozone by the vibrationally excited the OBrO radical. Finally, reaction 13a, which is fast, could be responsible for the low yield of the OBrO radical in method 2, in which the $OBrO^‡$ generated from reactions 5a and 5b further reacted with ozone, causing an overall low OBrO concentration in the reactor.

The mechanism proposed for laboratory production of OBrO may not be able to explain the atmospheric formation of OBrO. Since the atmospheric pressure is much higher than the total pressure of 1 Torr in our reactor, the $BrO^‡$ would have been quenched before colliding with another BrO or $BrO^‡$.

Moreover, though vibrationally excited OBrO could react with ozone, this chemistry may not have much direct impact on the stratospheric ozone since the $OBrO^‡$, if ever produced in the atmosphere, would be promptly quenched before colliding with ozone molecules. OBrO in the ground state has been found to be not very reactive toward ozone, suggesting that the OBrO may not participate directly in ozone destruction. But the understanding of the role of the OBrO in affecting the stratospheric ozone layer requires more studies aimed at understanding the photolysis of the OBrO radical and the coupling of ozone-affecting chemical processes with OBrO chemistry. The reactions of the OBrO radical with other atmospheric species, such as $NO_x$, $ClO_x$, and $HO_x$, are currently being examined in our laboratory.

## IV. Summary

The OBrO radical has been formed by three methods in a discharge flow reactor: (1) O + $Br_2$, (2) Br + $O_3$, and (3) microwave discharge of a $Br_2/O_2$/He mixture; the OBrO radical was detected with a mass spectrometer at $m/e = 111/113$. A new mechanism involving the vibrationally excited BrO self-reaction has been proposed to account for the formation of the OBrO. The OBrO generated thus could also be vibrationally excited. The OBrO in the ground state was found to be not very reactive to ozone, and the rate constant for reaction of the ground-state OBrO with ozone was estimated to be $k_{13} \leq 5 \times 10^{-16}$ cm$^3$ molecule$^{-1}$ s$^{-1}$. The vibrationally excited OBrO, on the other hand, is at least 3 orders of magnitude more reactive toward ozone than the ground-state OBrO, with a rate constant of $k_{13a} = (5.4 \pm 2.7) \times 10^{-13}$ cm$^3$ molecule$^{-1}$ s$^{-1}$ at 298 K.

**Acknowledgment.** The author thanks Prof. J. S. Francisco, Dr. S. P. Sander, Dr. K. O. Patten, and Prof. L. T. Chu for helpful discussions. This work was supported in part by the start-up fund from the UIUC Campus Research Board, by an EPA research grant (X825967-01-0 EPA), and by the National Science Foundation (NSF ATM-9813331).

## References and Notes

(1) Renard, J. B.; Lefevre, F.; Pirre, M.; Robert, C.; Huguenin, D. *C. R. Acad. Sci. Ser. II: Sci. TERRE Planetes* **1997**, *325*, 921.
(2) Renard, J. B.; Pirre, M.; Robert, C.; Huguenin, D. *J. Geophys. Res.* **1998**, *103*, 25383.
(3) Tevault, D. E.; Walker, N.; Smardzewski, R. R.; Fox, W. B. *J. Phys. Chem.* **1978**, *82*, 2733.
(4) Butkovskaya, N. I.; Morozov, I. I.; Tal'rose, V. L.; Vasiliev, E. S. *Chem. Phys.* **1983**, *79*, 21.
(5) Rattigan, O. V.; Jones, R. L.; Cox, R. A. *Chem. Phys. Lett.* **1994**, *230*, 121−126.
(6) Rattigan, O. V.; Cox, R. A.; Jones, R. L. *J. Chem. Faraday Trans.* **1995**, *91*, 4189.
(7) Kölm, J.; Engdahl, A.; Schrems, O.; Nelander, B. A. *Chem. Phys.* **1997**, *214*, 313.
(8) Miller, C.; Nickolaisen, S. L.; Francisco, J. S.; Sander, S. P. *J. Chem. Phys.* **1997**, *107*, 2300.
(9) Muller H. S. P.; Miller, C. E.; Cohen, E. A. *Angew. Chem., Int. Ed. Engl*. **1996**, *35*, 2129.
(10) Muller, H. S. P.; Miller, C. E.; Cohen, E. A. *J. Chem. Phys*. **1997**, *107*, 8292.
(11) Lee, T. J. *J. Phys. Chem.* **1995**, *99*, 15074.
(12) Pacios, L. F.; Gomez, P. C. *J. Phys. Chem.* **1997**, *101* (1 A), 1767.

(13) DeMore, W. B.; Sander, S. P.; Golden, D. H.; Hampson, R. F.; Kurylo, M. J.; Howard, C. J.; Ravishankara, A. R.; Kolb, C. E.; Molina, M. J. *Chemical Kinetics and Photochemical Data for Use in Stratospheric Modeling*, Evaluation Number 11, JPL Publication 97-4, Jet Propulsion Laboratory, California Institute of Technology, Pasadena, CA, 1997.

(14) Bedjanian, Y.; Le bras, G.; Poulet, G. *Chem. Phys. Lett*. **1997**, *266*, 233.

(15) Workman, M. A.; Francisco, J. S. *Chem. Phys. Lett*. **1998**, *293*, 65.

(16) Li, Z.; Freidl, R. R.; Sander, S. P. *J. Chem. Soc., Faraday Trans.* **1997**, *93*, 2683.

(17) Rowley, D. M.; Harwood: M. H.; Freshwater, R. A.; Jones, R. L. *J. Phys. Chem.* **1996**, *100*, 3020.

(18) Deters, B.; Burrows, J. P.; Orphal, J. *J. Geophys. Res.* **1998**, *103*, 3563.

(19) Brown, R. L. *J. Res. Natl. Bur. Stand. (U.S.*) **1978**, *83*, 1.

(20) Howard, C. J. *J. Phys. Chem.* **1979**, *83*, 3.

(21) Friedl, R. R.; Sander, S. P. *J. Phys. Chem.* **1989**, *93*, 4756.

(22) *CRC Handbook of Chemistry and Physics*, 72nd ed.; Lide, D. R., Ed.; CRC Press: Boca Raton, FL, 1991−1992; pp 11−44.

(23) Li, Z.; Tao, Z. *Chem. Phys. Lett.*, submitted.

(24) Li, Z.; Chu, L. T. *Chem. Phys. Lett*., to be published.

(25) Thorn, R. P., Jr.; Monks, P. S.; Stief, L. J.; Kuo, S. C.; Zhang, Z.; Klemm, R. B.; *J. Phys. Chem*. **1996**, *100*, 12199.

(26) Orlando, J. J.; Burkholder, J. B. *J. Phys. Chem*. **1995**, *99*, 1143.

(27) Sander, S. P.; Watson, R. T. *J. Phys. Chem.* **1981**, *85*, 4000.

(28) Turnipseed, A. A.; Birks, J. W.; Calvert, J. G. *J. Phys. Chem*. **1994**, *98*, 4594.

(29) Lancar, I.; LeBras, G.; Poulet, G. *J. Chim. Phys.* **1993**, *90*, 1897.

(30) Jaffe, S.; Mainquist, W. K. *J. Phys. Chem*. **1980**, *84*, 3277.

(31) Cox, R. A.; Sheppard, D. W.; Stevens, M. P. *J. Photochem*. **1982**, *19*, 189.

(32) Mauldin, R. L., III; Wahner, A.; Ravishankara, A. P. *J. Phys. Chem.* **1993**, *97*, 7585.

(33) Harwood, M. W.; Rowley, D. M.; Cox, R. A.; Jones, R. L. *J. Phys. Chem. A* **1998**, *102*, 1790.

(34) Chase, M. W. *J. Phys. Chem. Ref. Data* **1996**, *25*, 1069.